

Compressive Sensing for Synthetic Aperture Sonar

Jason C. Isaacs, *Member IEEE*

Abstract— This work analyzes approaches to synthetic aperture sonar imaging based on the concept of compressive sensing and compressive sampling. In compressed sensing, a low-dimensional linear projection is used to acquire an efficient representation of a compressible signal directly using just a small number of measurements. The signal (and image) is then reconstructed by solving an inverse problem by linear programming. It will be demonstrated that compressed sensing allows for improvements in synthetic aperture sonar systems by potentially reducing array sizes, beamforming computational requirements, synthetic array sampling requirements, image storage limitations, and allow for increasing vehicle speed. Results show that low error rates are feasible with several compressive sensing algorithms.

I. INTRODUCTION

Recent papers [3], [4], [5], and [6] have introduced the concept known as compressive sensing (CS) or compressive sampling. The basic principle is that sparse or compressible signals can be reconstructed from a surprisingly small number of linear measurements, provided that the measurements satisfy an incoherence property [3]. Such measurements can then be regarded as a compression of the original signal, which can be recovered if it is sufficiently compressible. A few of the many potential applications are synthetic aperture radar [1] medical image reconstruction [12], image acquisition [15], and sensor networks [9].

In [1] Baraniuk and Steeghs introduced the concept of compressive sensing for synthetic aperture radar (SAR). They showed that it was possible to reduce the computational requirements of SAR by utilizing the concepts from CS. The results presented in their paper showed processing capabilities for reduced sampling and elimination of the match filtering step in the formation of SAR imagery. This work follows the aforementioned SAR results with a study on the use of CS for synthetic aperture sonar (SAS). The results of two experiments using CS show that CS has potential application for the SAS community; especially interesting is the reduced sampling burden for image formation.

II. COMPRESSIVE SENSING

Given an N -dimensional signal x that is sparsely representable in some basis $\{\psi_i\}$ that provides a K -sparse representation of x ; that is

$$x = \sum_{i=1}^N \theta_i \psi_i = \sum_{l=1}^K \theta(i_l) \psi_{i_l} \quad (1)$$

where x is a linear combination of K basis vectors chosen from $\{\psi_i\}$, $\{i_l\}$ are the indices of those vectors, and $\{\theta_i\}$ are the weighting coefficients. We can create a sparsity basis matrix $\Psi = [\psi_1] \cdots [\psi_N]$, thus we have

$$x = \Psi \theta \quad (2)$$

where θ is an $N \times 1$ column vector with K nonzero elements. If the goal is to reconstruct sparse signals from measurements, a natural approach is to find the sparsest signal consistent with the measurements. Let Φ be a $M \times N$ measurement matrix, and $\Phi x = y$ the vector of M measurements of an N -dimensional signal x with $M < N$. Then the approach would be to solve the following optimization problem:

$$\min_x \|x\|_0, \text{ subject to } \Phi x = y \quad (3)$$

Here, the l_0 -norm $\|\cdot\|_0$ simply counts the number of nonzero components. This is not a norm in the strictest sense; nevertheless it is an effective way to solve the problem. However, solving (3) is a provably NP-hard problem [2]. Therefore, a result from Candes and Tao [3] demonstrates that a solution can be found for random Gaussian measurements Φ by solving the following optimization problem with $\|x\|_0 = K$:

$$\min_x \|x\|_1, \text{ subject to } \Phi x = y \quad (4)$$

provided $M \geq CK \log(N/K)$ for some constant C . CS theory tells us that when the matrix $\Upsilon = \Phi \Psi$ has the restricted isometry property (RIP) [3], [4], and [5] then it is

Manuscript received August 10, 2010.

Jason C. Isaacs is with the Naval Surface Warfare Center, Panama City FL 32407 USA (e-mail: jason.c.isaacs1@navy.mil.)

Approved for Public Release; distribution is unlimited.

possible to recover the K largest $\{\theta_i\}$ from a set of M measurements y . Adherence to RIP is similar to saying that Φ and Ψ are incoherent. Typically, Φ is chosen as an i.i.d. Bernoulli or Gaussian random variable matrix, as stated above. When RIP holds the signal x can be recovered from its coefficients θ exactly from y by solving (4) [3], [4]

The RIP has been proposed as a measure of the fitness of the matrix Υ . RIP is defined as follows: The K -restricted isometry constant for the matrix Υ , denoted by δ_K , is the smallest nonnegative number such that, for $\forall \theta \in \mathbb{R}^N$ with $\|\theta\|_0 = K$,

$$(1 - \delta_K) \|\theta\|_2^2 \leq \|\Upsilon \theta\|_2^2 \leq (1 + \delta_K) \|\theta\|_2^2 \quad (6)$$

A matrix has the RIP if $\delta_K > 0$; since calculating δ_K for a given matrix requires a combinatorial amount of computation, random matrices have been advocated.

CS is an efficient acquisition framework for signals that are sparse or compressible in a basis or frame Ψ . Rather than uniformly sampling the signal x , we measure inner products of the signal against a set of measurement vectors we then effectively compress the signal. By collecting the measurement vectors as rows of a measurement matrix this procedure can be written as $y = \Phi x = \Phi \Psi \theta$, with the vector y containing the CS measurements. Since $\Phi \Psi$ is a dimensionality reduction, it has a null space, and so infinitely many vectors x' yield the same recorded measurements y . Fortunately, standard sparse approximation algorithms (1) and (2) can be employed to recover the signal representation θ by finding a sparse approximation of y using the frame $\Upsilon = \Phi \Psi$.

III. COMPRESSIVE SENSING AND SAMPLING FOR SYNTHETIC APERTURE SONAR

Synthetic aperture sonar (SAS), is akin to SAR in that the aperture is formed artificially from received signals to give the appearance of a real aperture several times the size of the transmit/receive pair. SAS is performed by collecting a set of time domain signals and match filtering the signals to eliminate any coherence with the transmitted pulse. SAS images are generated by beamforming the time domain signals using techniques such as delay-and-sum, chirp-scaling, and the wave number method [11], which is used here.

The wave number beamforming process requires a number of FFT/IFFT pairs and is itself computationally complex. In order to alleviate this computational burden, experiments were performed with techniques for restoring SAS imagery in two ways, (1) by compressively sampling the number of channels that are beamformed and comparing that restored image with the original image and (2) by

increasing the sparsity of the raw signal data via a wavelet basis and performing a CS optimization on this resultant signal, beamforming the restored data, and comparing imaging results with the original image.

A. Sparse Sampling and Reconstruction without CS Optimization

The following experiments involve a reduction in data gained by sampling at 50% and 33.3% the channels of the sonar data. This is done in two ways, by uniform sampling and by randomly spaced sampling. Figure 1 below shows the differences in spacing between uniform and non-uniform compressive sampling with a 50% sparsity. The bottom example in Figure 1 is made using a Bernoulli random number generator to provide unequal spacing of various gap widths while maintaining a 50% sparsity requirement.

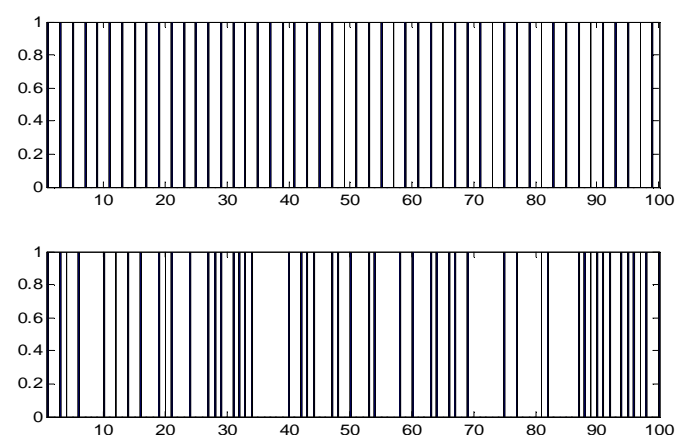


Fig. 1. Sample spacing example, top is uniform sampling (50 samples) and bottom is Bernoulli sampling with 51 samples.

Using these two sampling methods for sparsities of 50% and 66.7% experiments were run for image formation and reconstruction. Figures 2 and 3 below compare the results of 50% sparsity for both uniform and non-uniform compressive sampling. The raw data on the right in both figures was sampled accordingly and then beamformed to show the reconstructed image in the center. The image on the left is the original image formed by using the entire sample. As is demonstrated in Figure 2, there is a relatively low visual difference between the objects in both the original and reconstructed images. However, there is significant visual difference in the appearance of the background between these two images. This also holds true for the resultant images shown in Figures 3, 4, and 5. It may be that the compressive sampling of this signal captures larger structure information and misses the finer details of the background scatter. This loss of background resolution however may be an agreeable tradeoff for higher speed SAS systems.

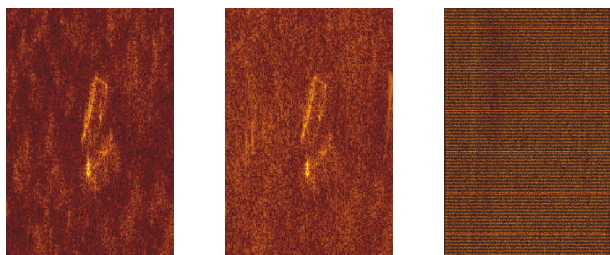


Fig. 2. Compressive sampling beamforming reconstruction example one. The original image is on the left and the reconstructed image is in the center with the sampled data on the right. The reconstructed image is formed from raw data that was uniformly sampled along track with 50% sparsity.

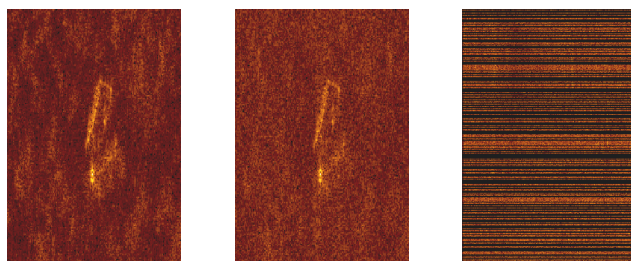


Fig. 3. Compressive sampling beamforming reconstruction example two. The original image is on the left and the reconstructed image is on the right. The reconstructed image is formed from raw data that was sparsely sampled along track with a Bernoulli sampling algorithm giving a sparsity of 50%.

The reconstruction errors for the results in Figures 2 and 3 are 1.542 and 0.691 respectively. The relative error is calculated as

$$E(x_0, x_1) = \|x_1 - x_0\|_2 / \|x_0\|_2 \quad (7)$$

where x_0 is the original image and x_1 is the reconstructed image, it must be noted that both the images and raw signal data are complex. Figures 4 and 5 below show the results from using 66.7% sparsity. The relative errors for reconstruction are 2.518 and 1.568 respectively. The error for the 66.7% non-uniform sampled reconstruction is on par with the uniformly sampled reconstruction at 50% sparsity.

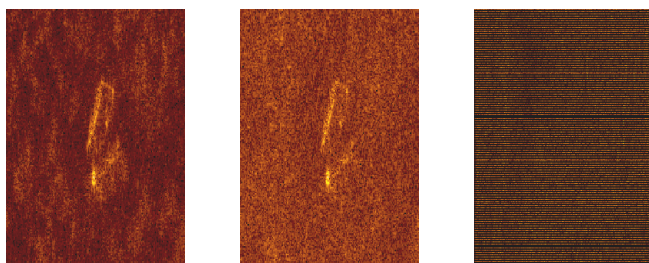


Fig. 4. Compressive sampling beamforming reconstruction example three. The original image is on the left and the reconstructed image is in the center with the sampled data on the

right. The reconstructed image is formed from raw data that was uniformly sampled along track with 66.7% sparsity.

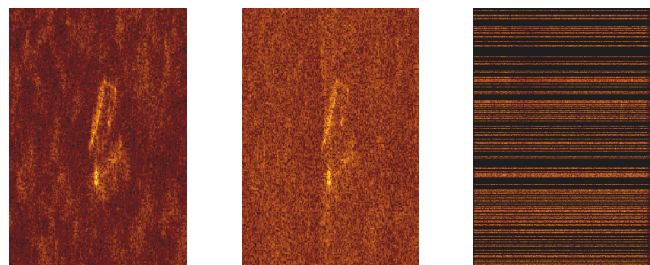


Fig. 5. Compressive sampling beamforming reconstruction example four. The original image is on the left and the reconstructed image is on the right. The reconstructed image is formed from raw data that was sparsely sampled along track with a Bernoulli sampling algorithm giving a sparsity of 66.7%.

As the results above demonstrate, the non-uniform compressive sampling method allows for a better reconstruction of the original data over traditional uniform sampling for the two experiments performed above. However, the compressive sampling method will perform poorly in highly detailed environments if the spacing is too large.

B. Sparse Sampling and Reconstruction with Compressive Sensing Optimization

The next step is to restore the original raw signal from the resulting compressively sampled signal by using methods of signal restoration from compressive sensing. Five such methods will be examined for reconstruction errors using the sampled raw signals versus the originals raw signals in image formation. The five algorithms are discussed briefly below, for a more thorough examination please see the references.

1) Iterative Hard Thresholding with FFT Basis

The Iterative Hard Thresholding (IHT) algorithm previously used in [2] is as follows. Let $x[0] = 0$ and use the iterative step

$$x^{[n+1]} = H_s(x^{[n]} + \Phi^T(y - x^{[n]})), \quad (8)$$

where $H_s(t)$ is the non-uniform operator that sets all but the largest (in magnitude) s elements of t to zero. If there is no unique such set, a set can be selected either at random or based upon some element ordering. The convergence of this algorithm was proven in [2] provided that $\|\Phi\|_2 < 1$. In this case (7) converges to a local minimum of

$$\min_x \|y - \Phi x\|_2^2 \text{ subject } \|x\|_0 \leq s. \quad (9)$$

2) Spectral Iterative Hard Thresholding with Periodogram and Music

In [10], Duarte and Baraniuk develop a new spectral compressive sensing theory for general frequency-sparse signals. The key ingredients are an over-sampled DFT frame, a signal model that inhibits closely spaced sinusoids, and classical sinusoid parameter estimation algorithms from the field of spectrum estimation. Using periodogram and eigen-analysis based spectrum estimates (e.g., MUSIC), their new algorithms perform comparably with other CS algorithms. They assume smooth or modulated signals that can be modeled as a linear combination of K sinusoids:

$$x[n] = \sum_{k=1}^K a_k e^{-j\omega_k n}, \quad (10)$$

where $\omega_k \in [0, 2\pi]$ are the sinusoid frequencies. In this work SIHTp and SIHTm will be used as acronyms for spectral iterative hard thresholding with periodogram and music respectively.

3) Min- l_1 with Equality Constraints

This method is also known as basis pursuit [3], [6], and [7] finds the vector with the smallest l_1 -norm as shown in (4). Instead of seeking sparse representations directly, basis pursuit seeks representations that minimize the l_1 -norm of the coefficients. By equating signal representation with l_1 -norm minimization, basis pursuit reduces signal representation to linear programming [6] and [7], which can be solved by standard methods. Furthermore, basis pursuit can compute sparse solutions in situations where greedy algorithms fail [7]. The results in [3] and [5] show that if a sufficiently sparse x_0 exists then this method will find it.

4) Total Variation with Equality Constraints

In Rudin et al. [14] the total variation norm: $TV(x) = \int_{\Omega} |\nabla x| dudv$ is proposed as a regularization functional that does not penalize discontinuities in the signal and thus allows for a better edge recovery. They formulate their technique as the constrained minimization problem,

$$\min_x \int_{\Omega} |\nabla x| dudv \quad \text{subject to} \quad \|x - x_0\|^2 = \sigma^2. \quad (12)$$

In this work, an additional constraint of equality is required, i.e. $\Phi x = y$.

The results of experiment (1) show that the reconstruction of compressively sampled data by beamforming results in low relative errors for 50% and 67% sparsity. Experiment (2) continues with the 50% compressively sampled data method from experiment (1) using non-uniform sampling, however prior to beamforming, the original data will be reconstructed using the four CS algorithms described above. In addition the data that comprises the images is four times as large. The results for experiment (2) show that the

combination of sampling fewer channels/pings and a sparse basis projection with CS reconstruction produce similar imagery to the original raw data. Figure 7 below shows the reconstructed images of experiment (2). The original raw data image formation result is shown in Figure 6 for comparison.

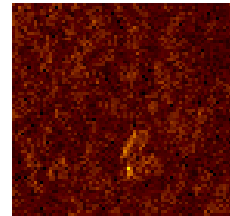


Fig. 6. Original beamformed image for experiment (2).

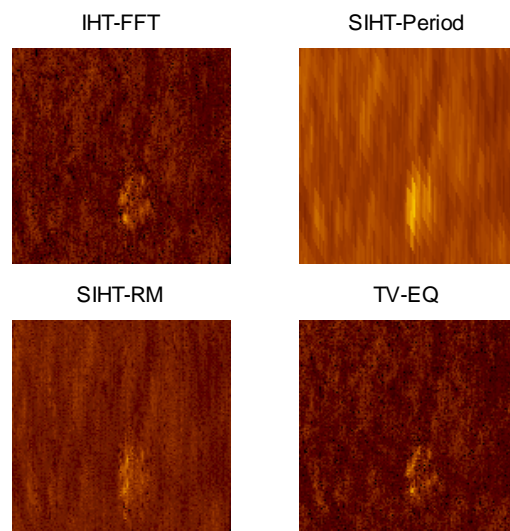


Fig. 7. Reconstruction results from uniform sampling the original raw data used to create the image in Figure 6. Clockwise from the top left the results are from IHT with FFT, SIHT with periodogram, SIHT with root music, and TV with equality constraints. The larger the SNR the better the reconstruction.

The relative reconstruction errors for the CS methods are 0.492 for IHT, 1.658 for SIHTp, 1.181 for SIHTm, and 0.390 for TV. As is demonstrated in Figure 7 the IHT and TV methods outperform the SIHT methods on this experiment. A visual inspection leaves little differences between the IHT, TV, and the original image. Most of those differences are in the background texture detail. The SIHT methods probably do poorly due to the density of the frequencies in the signals, since these methods rely on integral spaced spectral components. Future work with spectral methods could aim at frequency sampling at the receiver or possibly transmitting a frequency sparse signal to fully evaluate the restorative capabilities of SIHTp and SIHTm.

IV. CONCLUSION

The results above demonstrate experimental feasibility of compressive sensing for synthetic aperture sonar. The results are not lossless but show promise and may lead to a new

computationally efficient system for SAS processing. There are many different reconstruction algorithms. Each has its deficiencies and plusses depending on the sampling space. If the sampling is done in the time domain then it may be best to use a TV method. If the sampling is done in the spectral domain then maybe future work would show that SIHT with Music to be better than the others for reconstruction. As for the unevenly spaced sampling example, it appears that measurements at non-uniform intervals allow for better reconstruction due to the possibility of more detail information at some locations with high density sampling. These results could lay as a foundation for future work on the development of lower cost higher speed SAS systems. However, future work should be done to analyze the effects of the number of measurements and the bounds of the measurement matrix on the error of reconstruction for a system to be truly realizable.

ACKNOWLEDGMENT

This work was supported jointly by the NSWC PC ILIR research program and the Office of Naval Research.

REFERENCES

- [1] Baraniuk, R. and Steeghs, P., "Synthetic aperture radar," *IEEE Radar Conference*, Boston, 2007.
- [2] Blumensath, T. and Davies, M., "Iterative thresholding for sparse approximations," *Journal of Fourier Analysis and Applications* 14 (5) (2008) 629–654.
- [3] Candes E.J. and Romberg J., "Sparsity and incoherence in compressive sampling," *Inverse Problems* 23 969–985, 2007.
- [4] Candes E.J. and Tao T., "Near optimal signal recovery from random projections: universal encoding strategies?," *IEEE Trans. Inf. Theory* 52 5406–5425, 2006.
- [5] Candes E.J., Romberg J. and Tao T., "Robust uncertainty principles: Exact signal reconstruction from highly incomplete frequency information," *IEEE Trans. Inf. Theory* 52 489–509, 2006.
- [6] Chen, S.S. "Basis Pursuit," *PhD thesis*, Stanford University, Department of Statistics, 1995.
- [7] Chen, S.S., Donoho, D.L., and M.A. Saunders. "Atomic decomposition by basis pursuit." *SIAM Review*, 43(1):129–159, 2001.
- [8] Donoho D.L., "Compressed sensing," *IEEE Trans. Inf. Theory* 52 1289–1306, 2006.
- [9] Duarte M.F., Sarvotham S., Baron D., Wakin M.B., and Baraniuk R.G., "Distributed compressed sensing of jointly sparse signals," *39th Asilomar Conference on Signals, Systems and Computers* pp 1537–1541, 2005.
- [10] Duarte, M.F. and Baraniuk, R.G., "Spectral Compressive Sensing", *submitted for publication*, 2010.
- [11] Hawkins, D.W.; "Synthetic Aperture Imaging Algorithms: with application to wide bandwidth sonar," Ph.D. thesis, Univ. of Canterbury, Christchurch, New Zealand, 1996.
- [12] Lustig M., Santos J.M., Lee J.H., Donoho D.L. and Pauly J.M., "Application of compressed sensing for rapid MR imaging," *SPARS Rennes, France*, 2005.
- [13] Natarajan B.K., "Sparse approximate solutions to linear systems," *SIAM J. Comput.* 24 227–234, 1995.
- [14] Rudin, I., Osher, S., and Fatemi, E., "Nonlinear total variation based noise removal algorithms," *Physica D*, 60, pp 259–268, 1992.
- [15] Takhar D., Laska J.N., Wakin M.B., Duarte M.F., Baron D., Sarvotham S., Kelly K.F. and Baraniuk R.G., "A new compressive imaging camera architecture using optical-domain compression," *Computational Imaging IV - Proceedings of SPIE-IS and T Electronic Imaging* Vol 6065, 2005.